Earthquake Geotechnical Engineering for Protection and Development of Environment and Constructions – Silvestri & Moraci (Eds)
© 2019 Associazione Geotecnica Italiana, Rome, Italy, ISBN 978-0-367-14328-2

Nonlinear seismic site response analysis of soft clay deposits using SANICLAY-B constitutive model

G. Seidalinov
Fugro Germany Land GmbH, Berlin, Germany

M. Taiebat
The University of British Columbia, Vancouver, Canada

ABSTRACT: Natural clays exhibit complex response when subjected to earthquake induced cyclic loadings. A realistic modeling of such soil requires an appropriate representation of stress–strain relationship described by a constitutive model. An existing Simple ANIsotropic CLAY plasticity model with the Bounding surface formulation, SANICLAY-B, is used in this paper to represent such stress-strain relationship. The model performance is demonstrated first in reproduction of stress-strain response in undrained cyclic triaxial test, and modulus reduction and damping variation with shear strain in undrained cyclic direct simple shear test. A hypothetical soil column with initially normally and overconsolidated stress states is then used in nonlinear seismic site response analysis for a range of input peak ground accelerations. The results suggest that ground amplification is less pronounced with increasing PGA. The amplifications are larger for initially overconsolidated state than for normally consolidated at periods $T < 2$sec with the opposite trend at $T > 2$sec.

1 INTRODUCTION

Seismic site response analysis (SSRA) is required to understand local site effects for reliable seismic design of onshore and offshore structures. The analysis requires realistic representation of nonlinear dynamic soil properties. Engineering practitioners have been utilizing 1D equivalent linear analysis where the nonlinear dynamic properties of soil are represented by means of shear modulus reduction and damping ratio with an equivalent level of shear strain. Such curves have been established for a wide range of different soil types and are readily available.

With the advances in nonlinear constitutive models for soils, a true nonlinear SSRA becomes increasingly popular. It has been demonstrated for strong ground motions, for example by Yoshida & Iai (1998), that the true nonlinear SSRA is more reliable than the equivalent linear for a wide range of peak ground accelerations (PGA). The accuracy of a true nonlinear effective stress analysis however strongly depends on the capabilities of a constitutive model, utilized in the analysis, to properly represent stress-strain response of soil subjected to seismic loading. This motivates researchers to develop constitutive models based on observations made during the cyclic laboratory tests.

In this paper, an existing Simple ANIsotropic CLAY plasticity model with Bounding surface formulation (SANICLAY-B) proposed by Seidalinov & Taiebat (2014) is used in nonlinear SSRA. The model builds upon a successful hierarchical advancement of the SANICLAY family models. The developments started with the addition of anisotropy into a well-known Modified Cam-Clay model (Roscoe & Burland 1968) on the basis of work dissipation assumption by Dafalias (1986). Later non-associative flow rule was adopted by Dafalias et al. (2006) for more realistic stress-strain representation of clay behavior in monotonic tests. Destructuration mechanism was then introduced into the model by Taiebat et al. (2010) to replicate loss of structure observed in structured clays. SANICLAY-B model adopts the bounding surface formulation with additional

features required or more realistic representation of stress-strain response of clay subjected to cyclic loading. The model was validated against Georgia kaolin, structured Cloverdale, Ariake, and Gulf of Mexico clays in cyclic loading tests, including more recent validation in multi-directional cyclic shear tests in Yang et al. (2018). This provides the basis for model's capabilities in representation of the stress-strain response and for its further application in nonlinear SSRA.

Formulation of the model is briefly discussed with details on the most important model features required for realistic cyclic loading simulations. Model performance is then illustrated in the reproduction of stress-strain response against undrained cyclic triaxial test on Georgia kaolin clay and the corresponding modulus reduction and damping curves. Nonlinear SSRA is then presented illustrating the effect of increasing PGA and addition of destructuration parameters.

2 MODEL FORMULATION

The model is formulated in the stress space and consists of the bounding surface, plastic potential, and critical stress ratio surface. Complete SANICLAY-B model formulation is not given in this paper, and only the bounding surface formulation is presented. Interested readers are referred to Seidalinov & Taiebat (2014) and Seidalinov (2018) for more detailed formulation.

The bounding surface formulation and additional features adopted in the model are required for more realistic representation of stress-strain response of clay in cyclic loading. The main ingredient of the bounding surface formulation is the modification of a plastic modulus K_p required for computation of plastic strain increment $\dot{\varepsilon}_p$. A damage parameter is an additional feature that is required for proper simulation of continuous stiffness degradation during cyclic loading. In addition, a projection center σ_c, required for projecting current stress σ onto the bounding surface $F = 0$ in order to obtain an image stress $\bar{\sigma}$, is updated during each instance of stress reversal for more realistic stress-strain response in the course of unloading and reloading. In order to keep the uniqueness of the image stress $\bar{\sigma}$, the projection center has to evolve with the expansion/contraction and rotation of the bounding surface. The details of the above bounding surface formulation and the additional features are presented below.

2.1 *Plastic modulus*

In SANICLAY-B model, the plastic modulus required for computation of plastic strain increment $\dot{\varepsilon}_p$ is given by

$$K_p = \bar{K}_p + \frac{hp_0^3}{\langle b/(b-1) - s \rangle}; \qquad \bar{K}_p = -\left(\frac{\partial F}{\partial p_0}\bar{p}_0 + \frac{\partial F}{\partial \alpha} : \bar{\alpha}\right) \tag{1}$$

where $\bar{K}_p$ is a plastic modulus at the image stress with p_0 and α representing isotropic and rotational hardening of the bounding surface $F = 0$, h is a hardening function expressed as $h = h_0/(1 + d)$ with h_0 a model constant and d a damage parameter, p_0^3 is used to make the corresponding term having the same units as $\bar{K}_p$, b is a similarity ratio between the size of the bounding surface and the size of the loading surface passing through the stress state and homologous to the bounding surface with the projection center serving as the center of homology, s is an indirect measure of the size of the elastic nucleus and is set to be equal to 1 implying zero elastic range.

The essence of the bounding surface formulation is represented in eq. 1 in which the plastic modulus is computed for the stress states at and inside the bounding surface. At the bounding surface, the second term of the equation is equal to 0 and $K_p = \bar{K}_p$ with $\bar{K}_p$ representing the classical elastoplastic plastic modulus computed based on the consistency condition requiring the stress state to lie on the yield surface (replaced by the bounding surface in the bounding surface formulation). Inside the surface, the second terms is active and $K_p > \bar{K}_p$ thereby allowing computation of plastic strain increments within the bounding surface. Inside the bounding surface the consistency condition is not required to be satisfied

and therefore the parameter d entering the equation for h is an internal variable which does not enter $\bar{K}_p$ equation. The evolution of the damage parameter is activated at the beginning of cyclic loading and is given by

$$\dot{d} = a_d [(2/3)\dot{\mathbf{e}}^p : \dot{\mathbf{e}}^p]^{1/2} \tag{2}$$

where a_d controls the rate of damage evolution with the accumulation of plastic deviatoric strain, and $\dot{\mathbf{e}}^p$ is a plastic deviatoric strain tensor.

2.2 *Evolution of projection center*

The evolution of the projection center σ_c is given by the evolution of its deviatoric $\mathbf{s}_c$ and hydrostatic $p_c\mathbf{I}$ counterparts as

$$\dot{\mathbf{s}}_c = \frac{\mathbf{s}_c}{p_0}\dot{p}_0 + p_c\underline{\alpha}\left[-X\frac{\sqrt{3/2}p_c(p_0 - p_c)\boldsymbol{\alpha} : \dot{\boldsymbol{\alpha}}}{[(N^2 - (3/2)\boldsymbol{\alpha} : \boldsymbol{\alpha})p_c(p_0 - p_c)]^{1/2}}\mathbf{n}_c\right], \qquad \dot{p}_c = \frac{p_c}{p_0}\dot{p}_0 \tag{3}$$

in which X is a fixed number obtained at the instance of stress reversal (creation of PC), and $\mathbf{n}_c = (\mathbf{s}_c - \mathbf{s}_\alpha)/[(\mathbf{s}_c - \mathbf{s}_\alpha) : (\mathbf{s}_c - \mathbf{s}_\alpha)]^{1/2}$ with $\mathbf{s}_\alpha = p_c\alpha$.

The X is given, at the instance of stress reversal, by

$$X = \frac{[(\mathbf{s}_c - \mathbf{s}_\alpha) : (\mathbf{s}_c - \mathbf{s}_\alpha)]^{1/2}}{[(\mathbf{s}_b - \mathbf{s}_\alpha) : (\mathbf{s}_b - \mathbf{s}_\alpha)]^{1/2}}; \tag{4a}$$

$$\mathbf{s}_b = \mathbf{s}_\alpha + \mathbf{n}_c a_b, \quad a_b = \left[\frac{(N^2 - (3/2)\boldsymbol{\alpha} : \boldsymbol{\alpha})p_c(p_0 - p_c)}{(3/2)\mathbf{n}_c : \mathbf{n}_c}\right]^{1/2} \tag{4b}$$

3 MODEL PERFORMANCE IN SINGLE ELEMENT TESTS

Validation of SANICLAY-B model performance against a number of clays in undrained cyclic triaxial, direct simple shear, and multi-directional loading tests can be found in the works by Seidalinov & Taiebat (2014), and Yang et al. (2018). In this section, model performance for Georgia kaolin clay is briefly presented in terms of comparison with the experimentally observed stress-strain response in undrained cyclic triaxial loading, and comparison with typical modulus reduction and damping curves in undrained direct simple shear.

Table 1. Constants for Georgia Kaolin clay for single element tests and nonlinear seismic site response analysis.

Constants group	Designation	Value
Elasticity	κ	0.037
	v	0.2
Critical state	M_c	0.87
	M_e	0.86
	λ	0.121
Bounding surface	N	0.8
	h_0	50
	a_d	7
Rotational hardening	C	3
	x	1.69

Table 2. Initial values of internal variables for Georgia Kaolin clay for single element tests.

Model variable	Designation	Value
Size of bounding surface	p_0	1 kPa
Void ratio	e	1.5
Rotation of bounding surface	α	0
Stress state	(p, q)	$(1, 0)$ kPa

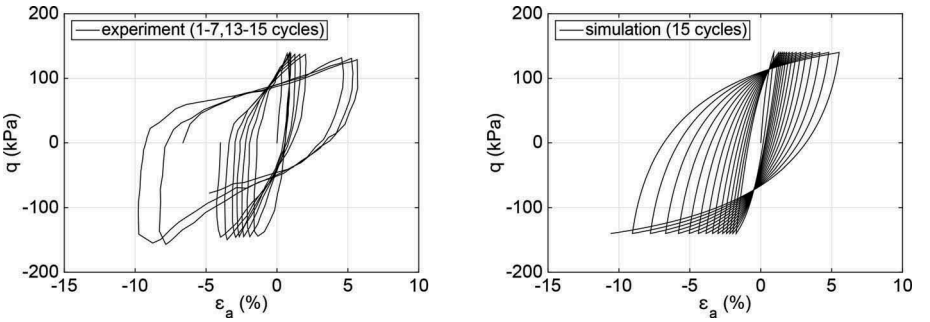

Figure 1. Undrained cyclic triaxial test on Georgia kaoling clay with applied cyclic stress amplitude $q_{cy} = 140.7$kPa.

3.1 *Parameters*

The model parameters used in this paper are previously calibrated by Seidalinov (2018) against experimental data by Sheu (1984) on Georgia kaolin clay. The model constants and initial internal variables are given in Tables 1 and 2, respectively. These parameters are to be used in this section for illustration of model performance.

3.2 *Undrained cyclic triaxial test*

Undrained cyclic triaxial loading tests on Georgia kaolin clay normally consolidated to $\sigma_c = 345$kPa are shown in Figure 1 for experimental and simulation results with cyclic stress amplitudes of $q_{cy} = 140.5$kPa. Prior to cyclic loading, isotropic consolidation to the σ_c is applied first in the simulations using the initial internal variables specified. The experimental data is available only for the specified cycles in the figure. This simulation result demonstrates that the model can replicate stress-strain response typically observed in the experiments. Additional three undrained cyclic triaxial simulation results with cyclic stress amplitudes of $q_{cy} = 121.4$, 136, and 165.5kPa are presented by Seidalinov & Taiebat (2014). The results suggest that SANICLAY-B model can replicate cyclic loading test results for a wide range of applied cyclic stress amplitudes using a single set of model parameters. This makes the model attractive for its application in nonlinear SSRA.

3.3 *Generating modulus reduction and damping variation*

Palmieri et al. (2017) demonstrated how SANICLAY-B model can be used to generate modulus reduction and damping variation with cyclic shear strain. A proper match with experimentally observed dynamic properties of clay was achieved using destructuration and bounding surface parameters. It is of interest to generate the dynamic properties using the model parameters calibrated against undrained cyclic triaxial test results on Georgia kaolin clay shown above. Prior to cyclic loading, K_0 consolidation to $\sigma_{vc} = 100$kPa is applied in the simulations using the initial internal variables specified above. Five cycles of the undrained cyclic direct simple shear test are then simulated for a range of cyclic shear strain amplitudes γ_{cy}. In the

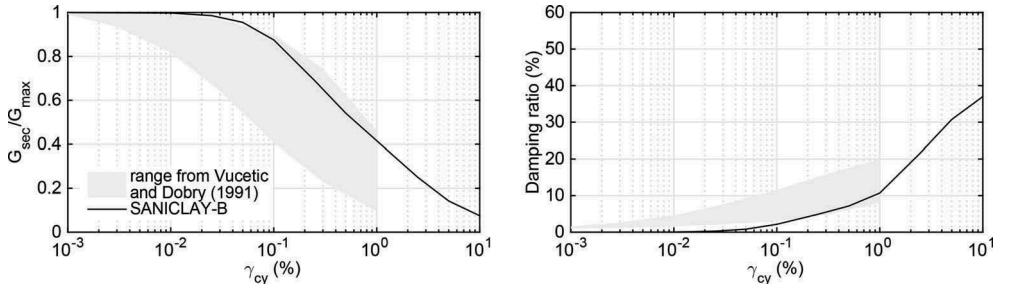

Figure 2. SANICLAY-B model simulations of modulus reduction and damping ratio variation with cyclic shear strain on soil samples K_0-consolidated to $\sigma_{vc} = 100$kPa.

range of $10^{-3}\% \leq \gamma_{cy} \leq 10^{1}\%$, secant shear modulus G and Damping ratio are then computed for the fifth cycle and the curves are constructed.

The results of the model simulations are shown in Figure 2 with solid lines. Typical experimental results summarized by Vucetic & Dobry (1991) for a range of different clays are also shown for reference in the figure for a number of clays with the range of $15\% \leq \text{PI} \leq 200\%$. The simulation results lie in the vicinity of the upper boundary for normalized secant shear modulus G_{sec}, and in the vicinity of the lower boundary for Damping ratio variations. These boundaries correspond to the experimental results for clays with the $\text{PI} = 200\%$, while Georgia kaolin is a clay with the $\text{PI} = 20\%$. More detailed investigations on this matter for experimental evidence and constitutive modeling are required in order to properly speculate on model's ability to generate dynamic properties of clay. Given that the model is calibrated independent of the typical modulus reduction damping curves, the model performance is considered satisfactory.

4 SEISMIC SITE RESPONSE ANALYSIS

SANICLAY-B model is implemented into OpenSEES finite element platform (McKenna et al. 2000) and used for the nonlinear SSRA. A soil column of 30m height with the water table at the surface of the column is assumed. Standard brick $u - p$ elements are chosen with three displacement and one pore pressure degrees of freedom per node. Two different overconsolidation ratio profiles shown in Figure 3 representing normally consolidated NC (dashed) and overconsolidated OC (solid) soil within the top 10m. Here we use a modified overconsolidation ratio (OCR_m) which is defined as $\|\sigma\|/\|\sigma_b\|$ with the σ_b obtained as a

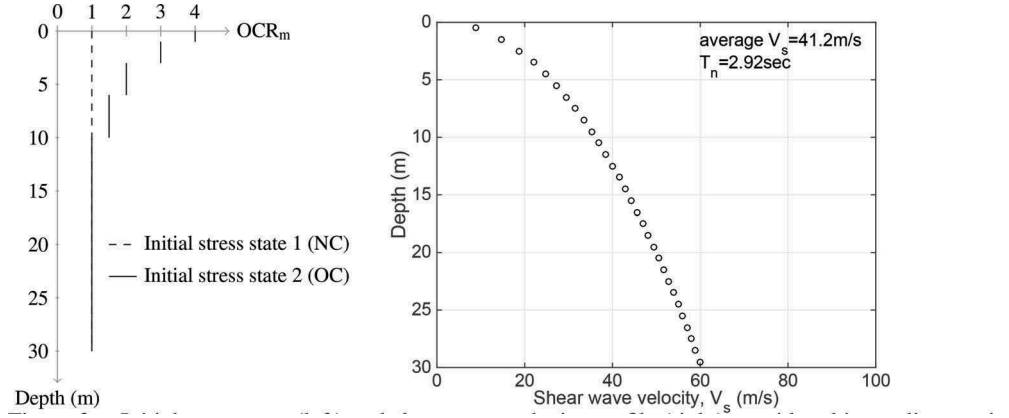

Figure 3. Initial state cases (left) and shear wave velocity profile (right) considered in nonlinear seismic site response analysis.

projection of the stress state σ onto the bounding surface. Given OCR_m and initial in-situ vertical stress, initial values of p_0 and e are assigned to SANICLAY-B model. Shear wave velocity profile with the velocities computed on the basis of SANICLAY-B model elastic shear moduli is also shown in Figure 3. The average $V_s = 41.2$m/sec corresponds to the natural

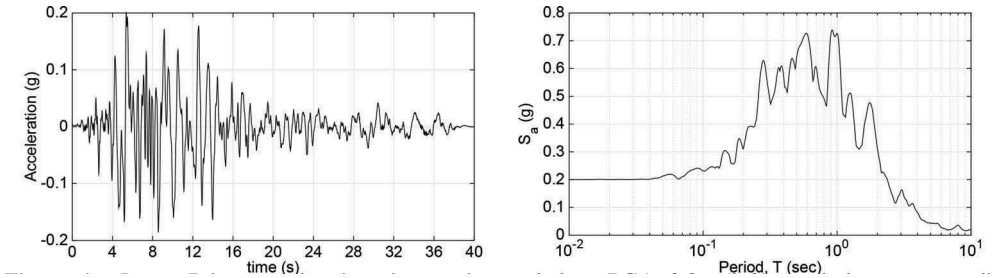

Figure 4. Loma Prieta acceleration time series scaled to PGA=0.2g (left), and the corresponding acceleration response spectrum (right).

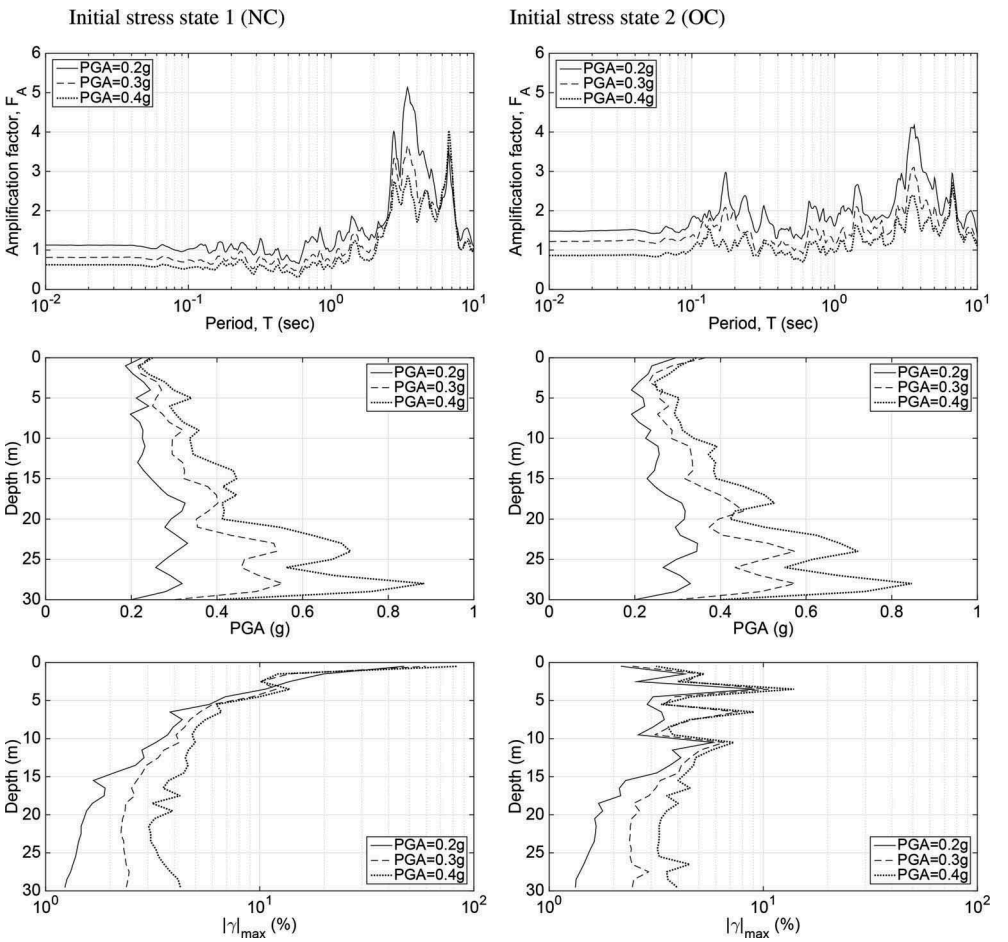

Figure 5. Simulated effect of peak ground acceleration for normally consolidated (left) and overconsolidated (OC) initial states.

period of soil column $T_n = 2.92$sec. Loma Prieta record shown in Figure 4 and scaled to different PGA values is applied at the rigid base of the column in the form of displacement motion thereby not requiring specification of the bedrock properties.

The results from nonlinear SSRA are shown in Figure 5. The Loma Prieta motion scaled to PGA = 0.2, 0.3, and 0.4g are used for the NC and OC initial states withing the considered soil column. The results are shown in terms of amplification factor F_A, and profiles of PGA and absolute value of maximum shear strain $|\gamma|_{max}$.

The amplification factor F_A tends to reduce with increased *PGA* value. Slightly larger F_A values can be observed for OC case at periods $T < 2$sec and smaller F_A values at $T > 2$sec. The PGA profiles for NC and OC cases appear to be not significantly different with larger values for larger input PGAs. Main difference is closer to the surface where slightly larger PGA values can be observed corresponding to larger amplification factors at lower periods. The absolute value of maximum shear strain $|\gamma|_{max}$ profiles are direct indication of a constitutive model performance. For NC and OC cases, the larger input PGA induces larger $|\gamma|_{max}$ throughout the depth of the soil column. Significant difference in the profile is observed within the top 10m. Very large $|\gamma|_{max}$ can be observed for the NC case which increase closer to the surface implying very soft response of clay. For the OC case the $|\gamma|_{max}$ values are significantly smaller but can still reach upto 14%.

5 CONCLUSION

SANICLAY-B model was previously developed and validated for its application in cyclic loading simulations. The performance of the model in generation of dynamic properties of clay is briefly demonstrated in this paper, and the model is then used in nonlinear SSRA for a hypothetical 30m soil column considering NC and OC initial states. The effect of PGA is studied showing that surface amplification reduces with the increased PGA as it causes larger deformations (i.e., larger plastic strains) and hence reduction of energy propagation toward the surface. It is also demonstrated that in OC case the amplifications are larger than for NC case at $T < 2$sec, while at $T > 2$sec the trend changes. Further research in simulating nonlinear seismic site effects for structured clay deposits is underway.

REFERENCES

Dafalias, Y. 1986. An anisotropic critical state soil plasticity model. *Mechanics Research Communications*, 13(6): 341-347.

Dafalias, Y. & Manzari, M. & Papadimitriou, A. 2006. SANICLAY: simple anisotropic clay plasticity model. *International Journal for Numerical and Analytical Methods in Geomechanics*, 30(12): 1231-1257.

McKenna, F. & Fenves, G. & Scott, M. 2000. Open System for Earthquake Engineering Simulation. *PACIFIC EARTHQUAKE ENGINEERING RESEARCH CENTER*.

Palmieri, F. & Seidalinov, G. & Taiebat, M. 2017. Exploring a bounding surface plasticity model in capturing the cyclic behavior of clays. In *Proceedings of The Seventies Canadian Geotechnical Conference*: Ottawa, Canada.

Roscoe, K. & Burland, J. 1968. On the generalised stress-strain behavior of "wet" clay. In Heymann & Leckie (eds), *Engineering Plasticity*, 53-609. Cambridge University Press.

Seidalinov, G. 2018. Constitutive and numerical modeling of clay subjected to cyclic loading. Ph.D. dissertation, University of British Columbia, Vancouver, Canada.

Seidalinov, G. & Taiebat, M. 2014. Bounding surface SANICLAY plasticity model for cyclic clay behavior. Ph.D. dissertation, University of British Columbia. Vancouver, Canada.

Sheu, W. 1984. Modeling of stress-strain-strength behavior of a clay under cyclic loading (Soil Dynamics). Ph.D. dissertation, University of Colorado. Boulder, Colorado, US.

Taiebat, M. & Dafalias, Y. & Peek, R. 2010. A destructuration theory and its application to SANICLAY model. *International Journal for Numerical and Analytical Methods in Geomechanics*, 34(10): 1009-1040.

Vucetic, M. & Dobry, R. 1991. Effect of soil plasticity on cyclic response. *Journal of Geotechnical Engineering*, 117(1): 89-107.

Yang, M. & Seidalinov, G. & Taiebat, M. 2018. Multidirectional cyclic shearing of clays and sands: Evaluation of two bounding surface plasticity models. *Soil Dynamics and Earthquake Engineering*, In Press.
Yoshida, N. & Iai, S. 1998. Nonlinear site response and its evaluation and prediction. In K. Irikura & K. Kudo & K. Okada & T. Sasatani (eds), *The Second International Symposium on the Effects of Surface Geology on Seismic Motion, Yokohama, Japan*: 71-90. Rotterdam: Balkema.